View Online / Journal Homepage / Table of Contents for this issue
Dynamic Article Links

Soft Matter

Cite this: *Soft Matter*, 2011, **7**, 9962

www.rsc.org/softmatter

PAPER

Surface grafting of thermoresponsive microgel nanoparticles†

Michael Seeber,[a] Bogdan Zdyrko,[a] Ruslan Burtovyy,[a] Taras Andrukh,[a] Chen-Chin Tsai,[a] Jeffery R. Owens,[b] Konstantin G. Kornev[a] and Igor Luzinov*[a]

Received 18th May 2011, Accepted 5th August 2011
DOI: 10.1039/c1sm05924f

Published on 30 August 2011 on http://pubs.rsc.org | doi:10.1039/C1SM05924F
Downloaded by Clemson University on 29 December 2011

A monolayer of thermoresponsive microgel nanoparticles, containing poly(*N*-isopropylacrylamide) (PNIPAM), has been anchored to the surface of silicon wafers, glass slides, polyvinylidene fluoride (PVDF) fibers, and tungsten wires using a "grafting to" approach. The behavior of the synthesized grafted layers is compared with the behavior of the PNIPAM brushes (densely end-grafted layers). The comparison demonstrates that in many aspects the microgel grafted layer is comparable to PNIPAM brushes with respect to its thermoresponsive properties. Indeed, the grafted monolayer swells and collapses reversibly at temperatures below and above the lower critical solution temperature (LCST) of PNIPAM. For the flat silicon substrate, a wettability study of the grafted layer shows an approximately 20° increase in the advancing contact angle of water upon heating above the LCST of PNIPAM. Wettability data obtained for the tungsten wires indicate that the grafted microgel layer retains its ability to undergo morphological changes when exposed to external temperature variations on complex curved surfaces. Therefore, the microgel-grafted layer can be considered as a system capable of competing with the PNIPAM brushes.

Introduction

Recent studies in the area of responsive surfaces/interfaces show their importance for prospective applications in micro- and nanofluidics, biocompatible materials, controlled drug release, nano- and biotribology, controlled cell growth and proliferation, and bio- and chemosensing.[1,2] A straightforward method to engineer the surfaces/interfaces of a substrate is *via* polymer grafting. In this method responsive macromolecules are covalently attached to a substrate boundary. Temperature,[3–5] light,[6–9] ultrasound,[10] electromagnetic fields,[11–13] and changes in the pH and ionic strength[14–18] of the environment can be used within these responsive systems as the physical and/or chemical stimuli for initiating controlled transformations of polymer chains. In this range, temperature-responsive polymers have attracted significant interest due to the relatively straightforward and precise methods available for temperature control. Additionally, many biological processes and their metabolic pathways are easily distinguished as a result of the accompanying variation in the temperature. Among the thermally responsive macromolecules, a great deal of attention has been paid to poly(*N*-isopropylacrylamide) (PNIPAM).[19–31] PNIPAM exhibits a temperature-sensitive phase transition in water, known as a lower critical solution temperature (LCST), at temperatures within the tolerances of human metabolism (~32 °C).[32] This is due primarily to the coil-to-globule transition at the critical temperature.[33] At temperatures below the LCST, PNIPAM macromolecules arrange into a swollen and hydrated conformation. Conversely, at temperatures above the LCST, PNIPAM chains collapse and arrange into a non-hydrated, collapsed conformation. Consequently, PNIPAM has been utilized in various forms, such as thermoresponsive hydrogels, particles, brushes, spheres and micelles.[1,2,34–38]

In general, covalent grafting of polymers, including PNIPAM, to a surface can be accomplished by "grafting from" or "grafting to" methods.[1,39–42] The "grafting from" technique involves polymerization that is initiated at the substrate surface by attached (usually covalently bonded) initiating groups. In contrast, the "grafting to" technique involves reaction of (end-) functionalized polymer molecules with complementary functional groups located on the surface, resulting in the formation of tethered chains. The major advantage of the "grafting to" method over other polymer attachment techniques is that well-defined polymers can be used for the grafting, resulting in the synthesis of well-defined grafted layers. Additionally, the grafting method is less-challenging from a chemical point of view, since it does not involve elaborate synthetic procedures. However, the low thickness (1–30 nm) of the layers obtained is a major shortcoming of this technique. In essence, "grafting to" is a self-limiting process because the polymer chains that are to be grafted must first diffuse through the existing polymer film to

[a]*School of Materials Science and Engineering, 161 Sirrine Hall, Clemson University, Clemson, SC, 29634, USA. E-mail: luzinov@clemson.edu*
[b]*Air Force Research Laboratory, Airbase Tech. Div., Airbase Sci. Branch, Tyndall AFB, Panama City, FL, 32403, USA*

† Electronic supplementary information (ESI) available: Detailed descriptions of temperature control of wetting of the wire. See DOI: 10.1039/c1sm05924f

This journal is © The Royal Society of Chemistry 2011

Published on 30 August 2011 on http://pubs.rsc.org | doi:10.1039/C1SM05924F
Downloaded by Clemson University on 29 December 2011

reach the reactive sites on the surface. This "excluded volume" barrier becomes more pronounced as the thickness of the tethered polymer layer increases.[43] To this end, the present manuscript reports a modification to the "grafting to" method that now allows the formation of much thicker, thermoresponsive PNIPAM-grafted layers. In essence, the proposed approach includes grafting of PNIPAM microgel nanoparticles containing reactive carboxyl (acrylic acid) groups to a surface. The straightforward nature and the facility of the "grafting to" approach is preserved in this case and the thickness of the grafted layer can be tuned by changing the size of the nanoparticles that are to be grafted. We compared the behavior of the synthesized grafted layers with the (reported in literature[44–47]) behavior of PNIPAM brushes (densely end-grafted layers). This comparison demonstrates that the microgel-grafted layer is comparable to PNIPAM brushes with respect to its thermoresponsive properties. Therefore, the microgel-grafted layer can be considered as a system capable of competing with the PNIPAM brushes.

Microgels are typically nano- or microparticles made of a cross-linked, hydrogel-forming polymer.[35,36] The microgel particles represent an intermediate between grafted polymer layers and macroscopic gels, thus combining some of the advantages of both. These advantages include: rapid phase transition, robustness, and having an easily tunable composition.[48] Microgel submicron particles, made of temperature-responsive polymers, have been widely researched for carrying out separations, as substrates for bioreactors, for enzyme and cell immobilization, as biosensors, and for *in vivo* drug delivery.[33,34,36,49–53] PNIPAM-containing microgels have been synthesized and functionalized using various techniques, such as emulsion non-surfactant or surfactant stabilized precipitation radical polymerization.[33,34,36,54,55] Complex microgel structures have also been fabricated. For example, PNIPAM hydrogels containing ferromagnetic nanoparticles have been synthesized.[56] Additionally, Huang *et al.* synthesized thermoresponsive and biodegradable microgels by copolymerizing NIPAM with dextran–lactate–2-hydroxyethyl methacrylate using an emulsion polymerization technique.[32]

In spite of the many potential applications for thin films made from microgels, most published work is devoted to the multilayered assemblies obtained by layer-by-layer techniques.[36] Only a few articles describe fabrication and investigation of microgel monolayers on a surface.[48,57,58] These studies describe the adsorbed layers and not the chemically anchored layers of microgel nanoparticles. The primary focus of the work reported in this paper is the synthesis and characterization of covalently grafted PNIPAM-containing microgel monolayers. To the best of our knowledge, fabrication of this type of grafted layer has not yet been reported in the scientific literature.

The synthesis of the microgels was conducted *via* a surfactant-stabilized free-radical-precipitation polymerization in an aqueous environment in the presence of acrylic acid as a co-monomer and *N*,*N*′-methylenebisacrylamide (BIS) as a cross-linker. The available carboxyl groups were then utilized to attach the microgels to the surface of various substrates, including silicon wafers, glass slides, tungsten wires, and poly(vinylidene fluoride) (PVDF) fibers. Surfaces were formerly activated by depositing a thin layer of poly(glycidyl methacrylate) (PGMA) as an anchoring layer.[59–61] This type of surface activation brings a significant number of epoxy groups to the substrate surface. Therefore, the microgel grafting was made possible through the reaction between epoxy groups from the PGMA anchoring layer and the carboxyl groups from acrylic acid.[59] The swelling and collapsing of the grafted microgel monolayers were investigated using atomic force microscopy (AFM) while scanning samples underwater at temperatures above and below the LCST. Scanning electron microscopy (SEM), AFM, contact angle measurements, elemental analysis, and proton NMR analyses were conducted to elucidate the structure, morphology, and surface characteristics of the synthesized microgels and the grafted layers.

Experimental

Materials

All reagents were used without further purification. 2,2′-Azobis (2-methylpropionamidine) dihydrochloride 97% (AAPH) and *N*, *N*′-methylenebisacrylamide 98% (BIS) were purchased from Aldrich. *N*-Isopropylacrylamide 99% (NIPAM) was purchased from TCI. *N*,*N*-Dimethylacetamide (DMA) 99% was purchased from Spectrum. Dodecyltrimethylammonium chloride (DTAC) 99.0% was purchased from Fluka and acrylic acid (AAc) 99.5% was purchased from Alfa Aesar. PGMA was synthesized radically according to published procedures.[61] In brief, glycidyl methacrylate (Sigma-Aldrich) was polymerized radically to give PGMA, $M_n = 135\,000$ g mol^{-1}, PDI = 2.97. The polymerization was carried out in methyl ethyl ketone (MEK, VWR) at 60 °C. Azobisisobutyronitrile, AIBN (Sigma-Aldrich), was used as an initiator. The resulting polymer was purified by multiple precipitations from MEK solution in diethyl ether. PGMA was labeled with Rhodamine-B *via* a reaction between the epoxy groups of the polymer and the carboxyl groups of the dye, as described elsewhere.[62] Tungsten wires were purchased from Small Parts.

PVDF fibers were fabricated by electrospinning using PVDF (M_n = 350–450 000 g mol^{-1}, purchased from Goodfellow) and poly(ethylene oxide) (PEO, $M_n = 1\,000\,000$ g mol^{-1} from Sigma-Aldrich). For this purpose, 2–3 mL of the polymer solution (0.2 g of PEO and 2 g of PVDF in 10 g of DMA (Spectrum)) were loaded into a 10 mL plastic syringe. The syringe was covered with a flexible heater (Watlow) (to maintain a constant temperature of 55 °C) and was attached to a syringe-type infusion pump. The syringe needle and the spinneret needle were connected using a Teflon tube. A stainless-steel spinneret needle was connected to a high-voltage device and the system was grounded to a collector. Nanofibers were collected with a copper fork and woven into yarns.

Instrumentation

A Veeco Dimensions 3100 Atomic Force Microscope (AFM), equipped with a Nanoscope 3A controller, was used to image the morphology of the grafted monolayers of the PNIPAM microgels in tapping mode. A silicon cantilever, with a force constant of 40 N m^{-1}, was used for the samples scanned in ambient air. Swelling and collapsing studies were conducted (in contact mode under water) using a Veeco Multimode AFM (with a Nanoscope 3A controller and a liquid cell) and silicon nitride cantilevers with

Published on 30 August 2011 on http://pubs.rsc.org | doi:10.1039/C1SM05924F
Downloaded by Clemson University on 29 December 2011

a force constant of 0.24 N m^{-1}. Monomer concentrations were monitored throughout the synthesis using a Bruker 300 MHz NMR. Elemental analyses of the synthesized nanogels were conducted using a Perkin–Elmer Series II-2400 CHNS/O Analyzer. Advancing and receding contact angle data were obtained on a Kruss (DSA10) fitted with a temperature-controlled sample cell. The water contact angle was determined using recorded video images of the drop's advancement and the drop's receding as water was added and removed from the drop with an automatic syringe. Still images were taken from the video using VideoDub freeware. ImageJ freeware was used to calculate the angles from the still images. Receding angles were determined using the angle tool function, while advancing contact angles were found using the Drop Shape Analysis plug-in for ImageJ. Scanning electron microscopy was conducted using a Field Emission Hitachi S4800 SEM. Ellipsometry measurements were obtained by using the InOm Tech Products, Inc., Model COMPEL ELC-11. Harrick Scientific Corporation (Model PDC-32G) plasma cleaner/sterilizer was used in the current study to treat PVDF fibers and tungsten wires prior to the grafting.

To investigate change in the surface energy of the substrate as a function of temperature, we ran two different experiments using tungsten wire modified with the grafted microgel layer. In the first experiment, the modified tungsten wire (130 μm) was placed into a thermo-insulated box with controllable humidity and temperature. Two alligator clips were attached to the wire ends thus closing the circuit when the device was connected to the power supply. The current and, therefore, the Joule heating of the wire can be controlled by adjusting the voltage. A different tungsten wire with a smaller (100 μm) diameter was used for the droplet delivery and deposition on the test wire. The delivery wire and droplet had the same temperature, as did the modified tungsten wire. In another experiment the grafted wire was attached to the 1D manipulator–positioner and gently dipped and held in the container with deionized water. A thermocouple was used to monitor and control water temperature. The experimental setup also consisted of a water pump that aided in the circulation of water through the jacket while also controlling the temperature. The thermocouple was used to accurately determine the temperature of the water. A 1D manipulator was used to move the modified substrate up or down. Last, a camera (Dalsa Falcon 1.4) was used to record the shape of the meniscus. To avoid diffraction from the edge of the water-jacketed condenser, the water was slightly overfilled. (Additional information on the experimental setup is provided in the ESI†.)

Synthesis of carboxyl-functionalized PNIPAM microgels

In general, we followed the modified procedure reported by Li *et al.*[63] so that 0.65 g (0.006 mol) of NIPAM, 5 mol% (2.87×10^{-4} mol) of AAc, 5 mol% (2.87×10^{-4} mol) of BIS, and 0.075 g (2.84×10^{-4} mol) of DTAC were dissolved in 60 mL of deionized H_2O and placed in a 100 mL three-necked round-bottom flask. The flask was equipped with an overhead mechanical stirrer set at 250 rpm, a nitrogen inlet and outlet, and a water-jacketed condenser. The monomer solution was placed in a water bath, thermostatted at 70 °C and bubbled with nitrogen for 1 hour to remove any dissolved oxygen. To initiate the polymerization, 0.03 g of AAPH was dissolved in 5 mL of water and charged into the flask. The solution was left to react for 6 hours under a nitrogen blanket. The reaction vessel was then submerged in an ice bath to arrest the polymerization. To purify the product, aliquots were centrifuged, decanted, and re-dispersed, first in fresh H_2O and then three times in tetrahydrofuran (THF, OmniSolv).

Grafting PNIPAM microgel nanoparticles to silicon wafers and glass slides

Highly polished single-crystal silicon wafers (Semiconductor Processing Co.) were first cleaned in an ultrasonic bath for 30 minutes, placed in a hot (80 °C) "piranha" solution (3 : 1 conc. H_2SO_4: 30% H_2O_2) for 1 hour, and then rinsed several times with high-purity DI water. (*As a precaution, it is important to note that the cleaning solution is highly corrosive and extremely reactive to organic substances.*) To deposit a thin layer of PGMA on the surface of the wafer, a 0.14% w/v solution of PGMA in chloroform (Spectrum) was made, and clean wafers were then coated by being dipped into the solution. Dip-coated wafers were annealed under vacuum at 120 °C for 20 min. After annealing, the wafers were rinsed three times for 10 minutes in fresh chloroform to remove any unattached polymer. Generally, this procedure produces a PGMA layer approximately 6 nm in thickness, as determined by ellipsometric measurements. A solution of approximately 6 mg mL^{-1} PNIPAM microgels in THF was used to deposit microgels onto the PGMA layer *via* the dip-coating procedure (Mayer Feintechnik D-3400, speed 240 mm min^{-1}). Typically, three consecutive dips were necessary to create a monolayer. Upon dip-coating, samples were annealed under vacuum at 120 °C for 2 hours. Samples were then rinsed three times for 10 minutes in fresh THF to remove any unattached particles from the surface. In an additional experiment, modified silicon wafers were left overnight in the solvent and it was determined that no grafted particles were lost. The procedure described above was also used to modify glass slides (VWR micro slides, 25 × 75 mm, 1.0 mm thick). The only difference was that in the modification of glass slides, the microgel nanoparticles were deposited onto the surface prior to the grafting by spin-coating (Headway Research) from THF suspension.

Grafting PNIPAM microgel nanoparticles to tungsten wires

Tungsten wires (130 μm in diameter) were first treated with air plasma for 10 minutes. The wires were then immersed in deionized water for 5 minutes (to develop surface hydroxyl groups) and air dried before deposition of the PGMA layer. Next, PGMA was drop-cast onto the wires from a 0.14% solution by weight of PGMA in chloroform. The wires were subsequently annealed at 120 °C under vacuum for 20 minutes. Following the annealing step, the wires were rinsed three times in fresh chloroform for 10 minutes to remove any unattached polymer from the surface. PNIPAM microgels were deposited onto the PGMA-modified tungsten wire from an approximately 0.4 weight percent solution in THF by drop-casting. Following this deposition, wires were then annealed for 12 hours at 120 °C under vacuum. Finally, the wires were rinsed three times in fresh THF for 10 minutes to remove any unattached particles from the wire surfaces.

This journal is © The Royal Society of Chemistry 2011

Published on 30 August 2011 on http://pubs.rsc.org | doi:10.1039/C1SM05924F
Downloaded by Clemson University on 29 December 2011

Grafting PNIPAM nanogels to PVDF fibers

In general, we followed the procedure reported for modification of PVDF membranes with a PGMA anchoring layer.[64] To activate the surface of PVDF the fibers were plasma treated for 3 minutes. Treated fibers were rinsed in MEK three times for 10 minutes and dried before deposition of the PGMA layer. For this purpose the fibers were first placed in a 0.14% w/v solution of PGMA in MEK. A round-bottom flask used in the experiment was equipped with a single-arm, screw-top vacuum attachment. Fibers in the PGMA solution were kept under vacuum until the solution boiled. This procedure was repeated three times. The vacuum procedure was used to fill the fiber/yarn pores with the PGMA solution. After drying, the fibers were annealed under vacuum at 60 °C for 2 hours. The PGMA-modified fibers were rinsed three times in fresh MEK to remove any unattached polymer from the surface. Fibers were then placed into a suspension of microgel nanoparticles in THF (6 mg mL^{-1}) and treated in the same fashion as they were for the PGMA modification. Modified fibers were then annealed under vacuum at 120 °C for 2 hours. The annealed fibers were again washed three times for 10 minutes in fresh THF to remove any free particles. All fibers used for SEM imaging were sputter-covered for one minute with platinum.

Determination of changes in the monomer concentration by proton NMR spectroscopy

For the NMR experiments, microgel particle synthesis was repeated using deuterium oxide (D_2O) as a solvent. Changes in the monomer concentration during synthesis were monitored. As an internal reference,[55] 40 μL of DMAC were added to the reaction mixture. Next, 1 mL aliquots were collected at time intervals of 0, 5, 10, 20, 40, 80, 120, and 240 min. This was accomplished by withdrawing approximately 1 mL of the reaction solution at each given time interval and quenching it in an ice bath to halt the polymerization. The monomer concentration was calculated from the integrated area of the peaks that are individually unique to each monomer, as opposed to the peaks observed for the DMAC. Concentration values were calculated as a ratio of initial concentration and the area under the respective bands.

Swelling and collapsing of the PNIPAM microgel layer monitored by AFM

Silicon wafers (1 × 1 cm) were grafted with PNIPAM-containing microgel nanoparticles and placed inside an AFM liquid cell mounted on a temperature-controllable stage. Samples were scored with a razor blade to locally remove particles from the surface. To observe conformational changes, scanning was conducted across the scratch to view the profile of the changing layer. Temperatures were fixed at 22 °C and 40 °C for the swelling and collapsing experiments, respectively. The AFM scanning was conducted using a force as small as possible, to minimize any lateral compression of the microgels. ImageJ freeware was used to extract the profile heights from the various scans.

Results and discussion

Microgel nanoparticles

Upon gentle heating of the nanoparticle suspensions a transition of the microgel particles from transparent at room temperature to opaque was observed as the suspension reached 35–40 °C. This transition was the first indicator that the nanoparticles exhibit thermoresponsive properties, since this transition occurred at just above the LCST temperature of pristine PNIPAM, which is typically 32 °C. Fig. 1 shows the SEM images of a drop-cast (from a 6–8 mg mL^{-1} particle suspension in THF) layer of microgels on a silicon wafer. The images confirm that, indeed, nanoparticles with a spherical shape were synthesized. The size of the particles, estimated from the image, is approximately 250 ± 20 nm.

The tentacle-like substance surrounding and connecting the particles indicates that the nanoparticles possess a core–shell structure. Scientific literature[58,65–72] well-documents the core–shell morphology of microgels prepared by precipitation–copolymerization of NIPAAM and a BIS cross-linker. The phenomenon is associated with the dissimilar copolymerization rates of BIS and NIPAAM. Specifically, the rate is higher for BIS, which is depleted early in the polymerization process. This situation causes formation of the highly cross-linked BIS-enriched cores of the microgel particles. Data on distribution of the AAc units in NIPAAM–BIS–AAc microgel nanoparticles are controversial.[65] Some researchers reported enrichment of the core with AAc fragments, whereas other scientists suggested that the shell contains higher concentration of AAc monomeric units.

To estimate distribution of the components in the particles synthesized in this work, we have determined consumption rates for the monomers during the polymerization. For this purpose, the composition of the polymerizing media was analyzed with proton NMR as a function of polymerization time. The results of the experiment are shown in Fig. 2. It is evident that, in our case, AAc and BIS monomers are consumed much more rapidly than NIPAM. In fact, AAc and BIS are fully consumed at approximately the 20 minute interval. Consequently, we can suggest that the cores of the particles are much more densely cross-linked with BIS and contain a higher ratio of AAc. Moreover, it can be assumed that, even though the nanoparticle synthesis was conducted for 6 hours, the formation of the microgels was practically complete in approximately 40 minutes.

Elemental analysis measurements were taken on the final microgels to estimate the amount of each monomer contained in the particles. From percentages of C, N, H and O, simultaneous

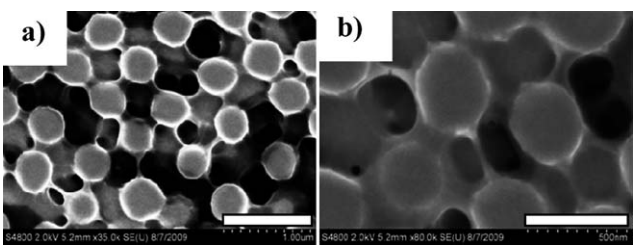

Fig. 1 SEM images of PNIPAM microgel nanoparticles drop-cast on a silicon wafer from diluted solution. Scale bar: 1 μm (a) and 500 nm (b).

Published on 30 August 2011 on http://pubs.rsc.org | doi:10.1039/C1SM05924F
Downloaded by Clemson University on 29 December 2011

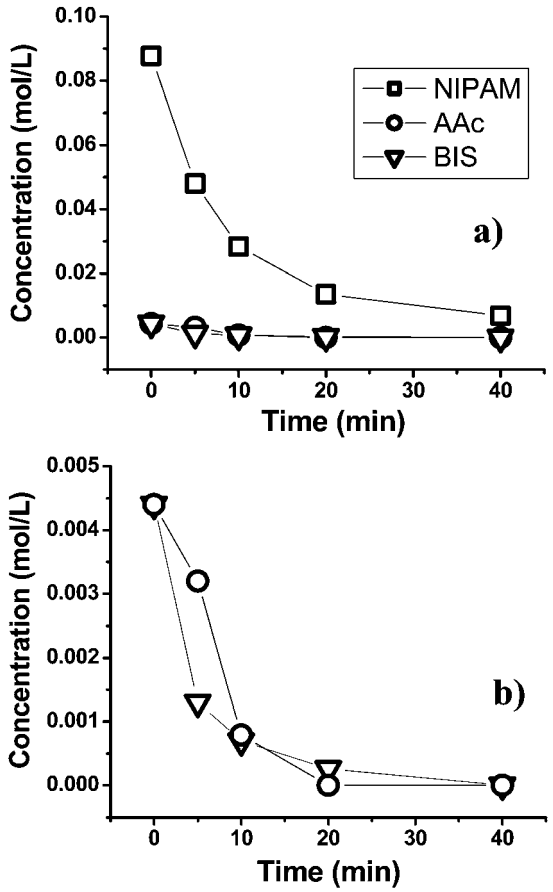

Fig. 2 Change in concentrations of monomers during the synthesis of microgel nanoparticles. (a) Change for NIPAM, AAc, and BIS. (b) Change for AAc and BIS only. The concentrations were determined by NMR.

mol fraction equations were used to determine the approximate weight percents of the individual monomers present in the microgel particles. Elemental analysis confirmed that NIPAM was the most abundant monomer in the final co-polymer (55%), and AAc and BIS comprised 21% and 24%, respectively. Coupled with the NMR results, this also suggested the presence of a densely cross-linked core with a high ratio of AAc and BIS and a shell with mostly NIPAM "hairs." Additionally, the obtained NMR and elemental analysis results indicated that, at the end of the polymerization, a PNIPAAM homopolymer was formed.

Grafting microgel nanoparticles

A thin layer of PGMA was deposited onto the surfaces of silicon wafers, glass slides, PVDF fibers, and tungsten wires for the initial surface modification. PGMA, which contains an epoxy group in every repeating unit, has been used extensively as a macromolecular anchoring layer for the grafting of polymers to surfaces.[59–61,73–76] A study of the deposition of PGMA onto various surfaces revealed that a uniform and homogeneous epoxy-containing layer can be obtained on surfaces using either adsorption, spin-coating, or dip-coating. The anchoring layer can be employed to modify various polymeric and inorganic surfaces. Therefore, procedures developed in this work for silicon, glass, PVDF, and tungsten surfaces can be readily adapted to other materials.

In our work, suspension in THF was used to deposit microgel nanoparticles onto substrates prior to the grafting. The organic solvent was employed instead of an aqueous environment to ensure the formation of a densely packed monolayer of the particles on a surface. Indeed, previous studies for microgels containing acrylic acid units suggested that close-packed microgel monolayers cannot be formed from water because of the strong ionic inter-particle repulsion originating from the dissociated AAc units.[48,58,77,78] Fig. 3a shows an AFM topography image for the "as deposited" monolayer of nanoparticles on the silicon wafer. The particles in the microgel monolayer are nearly monodisperse and close-packed into a periodic hexagonal-like structure. Next, the monolayer samples were annealed at 120 °C for 2 hours to conduct a reaction between the carboxylic groups of the AAc and the epoxy groups of the PGMA. Previously we demonstrated that, at this temperature, carboxy-terminated PNIPAM macromolecules can be readily grafted onto a surface *via* the PGMA anchoring layer.[79] The thickness of the grafted layer measured by ellipsometry was 58 ± 2 nm. After the grafting, the structure of the layer remained practically unchanged (Fig. 3b).

Fig. 4 shows that the grafted layer covers the silicon substrate uniformly at the microscopic level. The root mean square (RMS) roughness of the layer, evaluated from the topographical 10 × 10 μm AFM image (Fig. 4a), is 5.4 nm. The roughness, which is much lower than the layer thickness, confirmed the formation of a complete monolayer. Fig. 4c shows an SEM image taken at the edge of a silicon wafer to visualize a cross-sectional view of the surface. It is evident that the particles are attached to the surface and assume a "pancake" type of conformation.

The particle density of the grafted layer, estimated from counting the particle surface population, is ~9 particles per μm^2 (Fig. 4a). The center-to-center distance for the particles in the monolayer, measured from the main peak of the 2D Fourier transform of the AFM 10 × 10 μm topographical image (Fig. 4a), is 300 ± 25 nm. Since the thickness of the layer measured by ellipsometry is only 58 nm, the obtained data confirm that, in the grafted layer, the particles are flattened because of their interaction with the surface. Specifically, the nanoparticles in the dry monolayer adopt this morphology when the horizontal diameter is larger than the vertical. We measured

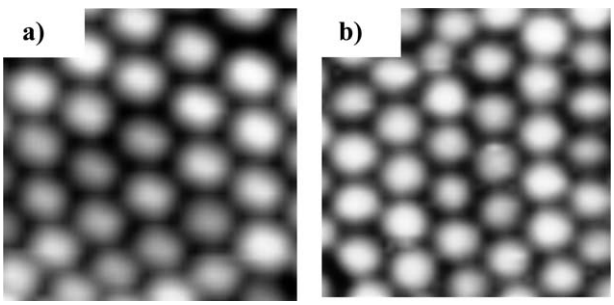

Fig. 3 AFM topography images (2 × 2 μm) of the microgel nanoparticle monolayer on a silicon wafer: (a) before grafting and (b) after grafting. Vertical scale 100 nm.

This journal is © The Royal Society of Chemistry 2011

Published on 30 August 2011 on http://pubs.rsc.org | doi:10.1039/C1SM05924F
Downloaded by Clemson University on 29 December 2011

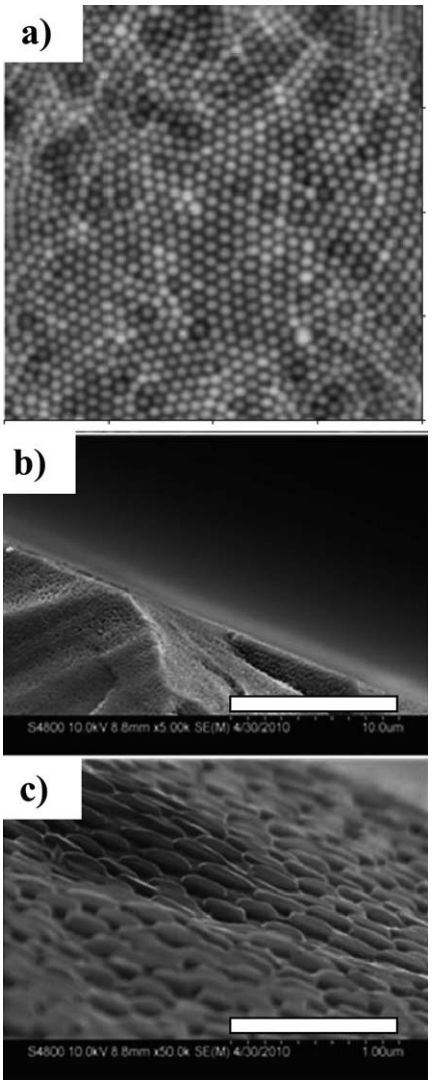

Fig. 4 a) AFM topographical image (10 × 10 μm) of the grafted microgel layer on silicon wafer, vertical scale: 150 nm. SEM images of grafted microgel layer on silicon wafer: (b) rough edge of the wafer, scale bar 10 μm; (c) close to the wafer edge, scale bar 1 μm.

the height of the 30 nanoparticles at the edge of the monolayer and found them to be 70 ± 7 nm. This result corroborates the conclusion drawn from the ellipsometric measurements, *i.e.*, the particles are squashed towards the surface in a "pancake-like" morphology. AFM data on the particle's height (h) and diameter (center-to-center distance, d) allowed for the estimation of the dry unperturbed particle size, using the volume of the spherical cap-shaped particles (V):[58,80]

$$V = \frac{1}{6}\pi h\left(3\left(\frac{d}{2}\right)^2 + h^2\right)$$

After the volume was found, the diameter of a spherical particle having the same volume was calculated. In this fashion, the dry-state diameter of the microgel particles was determined to be ~163 nm.

Fig. 4b, illustrating the rough edge of the silicon wafer covered with the grafted layer, indicates that the monolayer of particles can be attached to shapes more complex than simple flat silicon wafers and glass slides. In fact, we effectively modified tungsten wires with the microgel monolayer. The grafted layer covered the surface evenly and possessed virtually the same morphology as the layer grafted to the Si wafer (Fig. 5). Yarns of PVDF fibers (Fig. 6a and b) were covered with the microgel layer as well. In this case, we used Rhodamine B-labeled PGMA to visualize the attachment of the anchoring polymer layer to the fiber surface. Fluorescent microscopic imaging of the fibers confirmed PGMA attachment to the surface (Fig. 6c). A comparison of SEM images for the unmodified (Fig. 6a and b) and modified (Fig. 6d) fibers shows as well that the deposition of the anchoring layer was achieved. After the activation of the fibers, the nanoparticles were grafted onto their surface. SEM images of the fibers, after the modification with the particles, are shown in Fig. 6e and f. The images confirm the successful grafting of microgels to the surface. These images clearly show that the particles completely cover the curved surfaces of the fibers as well as the crevices and pores created between fibers in a monolayer fashion.

Swelling-collapsing of the grafted layer in water as a function of temperature

Due to surface confinement microgel particles can display different switching behavior than do free particles. Toward this end, AFM underwater studies were conducted to determine if the particles in the grafted monolayer demonstrate the ability to swell and collapse with temperature change. In this experiment, the layer was scratched with an ultra-sharp needle to delaminate the layer down to the Si-wafer. The sample was then scanned over the area with the scratch to observe the quality and thickness of the grafted monolayer. Fig. 7 shows AFM topographical images of the microgel layer near the scratch recorded at temperatures below (25 °C) and above (40 °C) the LCST of the PNIPAM in water. It is evident that the monolayer swells and collapses at the lower and higher temperature, respectively. The difference in the layer thicknesses when the microgels were collapsed and swollen was measured. For the grafted layer in the

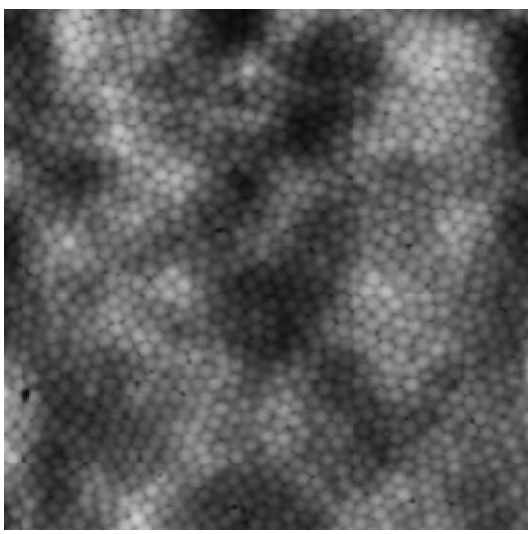

Fig. 5 AFM topographical image (10 × 10 μm) of the grafted microgel layer on tungsten wire, vertical scale: 200 nm.

Published on 30 August 2011 on http://pubs.rsc.org | doi:10.1039/C1SM05924F
Downloaded by Clemson University on 29 December 2011

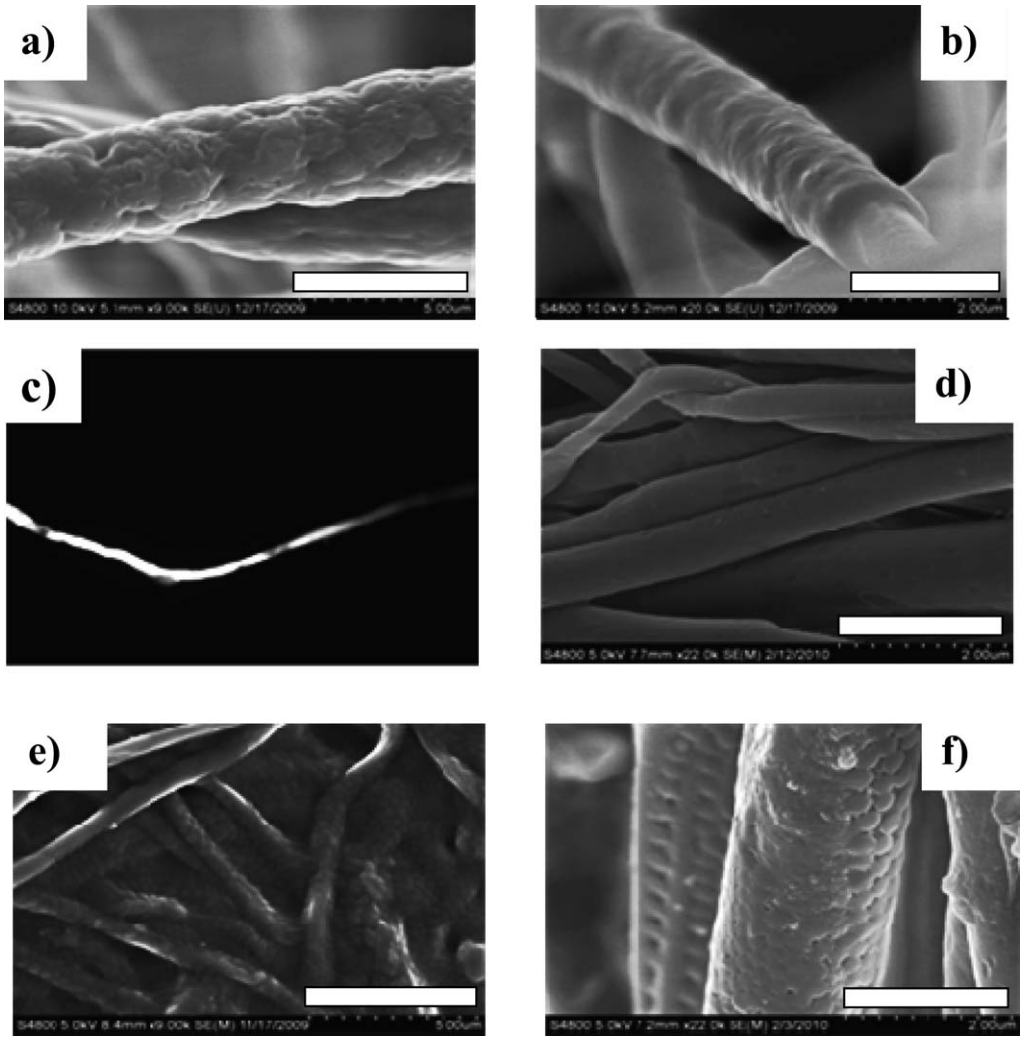

Fig. 6 a and b) SEM images of virgin PVDF fibers; (c) fluorescent microscopy image of fibers modified with Rhodamine-B-labeled PGMA; (d) SEM image of the PGMA-modified fibers; (e and f) SEM images of the fibers grafted with microgels. Scale bar: (a and e) 5 μm; (b, d and f) 2 μm.

collapsed state (Fig. 7b), this thickness was calculated to be ~214 nm and, while in its swollen state, the thickness was calculated to be ~468 nm (Fig. 7a). Therefore, the thickness of the grafted microgel layer increases ~2.2 times in the cold water. Since the grafted films extend in only the vertical direction upon crossing the LCST, the volume of the layer changed by a factor of ~2.2. The result indicates that ~272 mg m^{-2} of water can be absorbed and released by the layer upon swelling and collapsing, respectively.

A significant difference exists between the AFM thicknesses of the dry-grafted layer and the collapsed/swollen layer in water. In fact, the thickness of the dry-grafted layer, estimated from ellipsometry, is ~58 nm. The thickness of the collapsed layer is ~3.5 times higher. Therefore, the water content in the collapsed

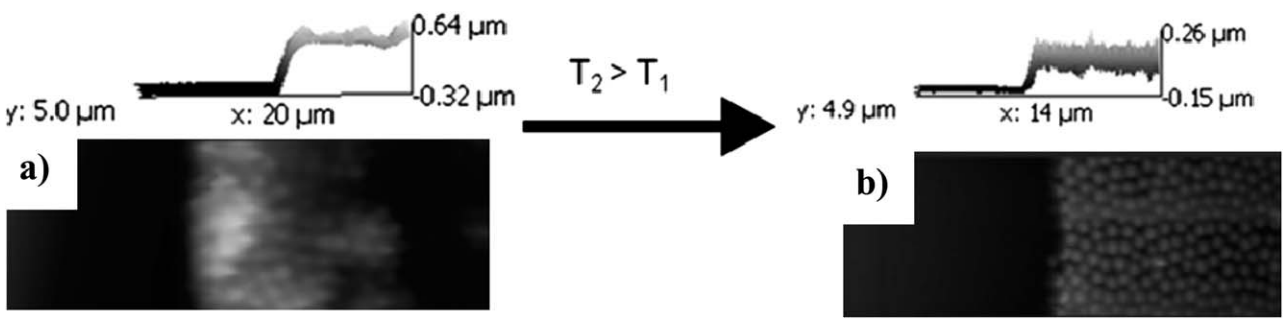

Fig. 7 AFM topographical images of the scratched grafted-microgel layer under water at temperatures below (a) and above (b) the LCST of PNIPAM.

 This journal is © The Royal Society of Chemistry 2011

Published on 30 August 2011 on http://pubs.rsc.org | doi:10.1039/C1SM05924F
Downloaded by Clemson University on 29 December 2011

layer is ~156 mg m^{-2} or on the order of 67%. For the swollen layer the water content is ~410 mg m^{-2} or 88%. The results obtained for the fractional water content are close to the data reported for PNIPAM microgel layers that are electrostatically adsorbed on a silicon surface modified with poly (ethyleneimine).[48]

It is appealing to compare the swelling capacity of the grafted microgel layer synthesized in this work with the swelling capacity of PNIPAM brushes. Kaholek *et al.* demonstrated that PNIPAM brushes, anchored by the "grafting from" approach to a flat surface, swelled ~3 times in room-temperature water compared to the dry state thickness of ~200 nm.[44] For the thinner (15 nm dry thickness) PNIPAM brush, obtained using the "grafting to" method, ~5 times swelling was reported.[45] Conversely, in room-temperature water, the microgel-grafted layer extended ~8 times in the vertical direction from the dry state. Therefore, in terms of reversibility and capacity, temperature-induced swelling of microgel-grafted layers can be considered, as a system, comparable to linear PNIPAM brushes with respect to their thermoresponsive properties.

Fig. 8 exhibits the repeatability of the swelling and collapsing of the grafted microgel layer. Three cycles of heating and cooling were performed. Cycles 1 and 2 at 25 °C were essentially equivalent. However, an increase in thickness was observed during the third cycle, which suggests that the equilibrium time for complete swelling might not have been reached within the first two cycles. At elevated temperatures, a general decrease in thickness was observed from Cycle 1 to Cycle 3. This also suggests that not enough time was given for the complete collapse and expelling of the water. To evaluate the robustness of the microgel layer upon the swelling–deswelling cycles, we subjected glass slides grafted with a PNIPAM nanoparticle layer to six heating–cooling cycles in water. The duration of each cycle was two hours: 1 hour at 20 °C and 1 hour at 50 °C. The experiment confirmed the noteworthy robustness of the layers, since no particle removal was observed *via* AFM imaging.

Wettability of the grafted microgel layers

An important property of the grafted PNIPAM layers is their ability to demonstrate temperature-dependent wettability.[46,47,81] Therefore, we further analyzed the microgel-grafted layer using contact angle measurements taken as a function of temperature.

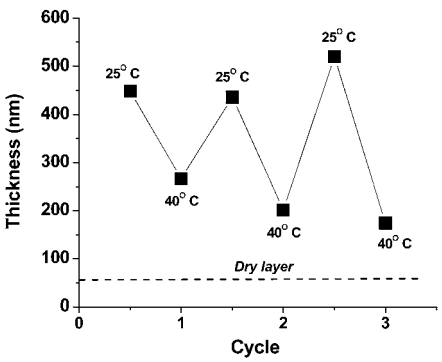

Fig. 8 AFM thickness of the grafted microgel layer under water at different temperatures.

First, advancing contact angles were determined, to confirm the transition of the surface covered with microgels from more hydrophilic to more hydrophobic in nature. For the measurements, silicon wafers grafted with the nanoparticles were placed inside a temperature-controlled sample cell. Water was continuously fed onto the surface from a needle close to the surface. As the volume of the drop increased, the drop spread and, therefore, it was exposed to the new surface. Video was taken and individual snapshots were captured at points where the drop spread (Fig. 9a and b).

At 23 °C, the advancing contact angle was measured to be 71 ± 2° (Fig. 9a). Upon heating to 50 °C, the advancing contact angle was determined to be 90.0 ± 2° (Fig. 9b). Hence, an approximately 20° increase in the contact angle is observed upon heating above the LCST of PNIPAM. Advancing angle temperature transitions in the similar range were found for the PNIPAM brushes.[46,47] This emphasizes that, analogous to the brushes made of end-grafted linear PNIPAM chains, cross-linked microgel nanoparticles, constituting the grafted layer, also have the ability to rearrange their conformation across the LCST and exhibit a wettability change due to a change in temperature. We also determined receding contact angles for the surface modified with the grafted microgels (Fig. 9c and d). A significant hysteresis was found to exist between the advancing and receding angles. Namely, the receding contact angles were measured to be 13 ± 2°. The angles were virtually independent from the temperature. The phenomenon was already reported for surfaces modified with PNIPAM-grafted layers.[47,81] The observed result indicates that the PNIPAM-containing microgel particles expose similar chemical groups to the water both below and above the LCST. This effect is also connected with significant water content in the swollen and the collapsed grafted layers.

Wettability measurements were conducted on the tungsten wires modified with the microgel-grafted layers. Fig. 10 shows two images of water droplets placed on the modified wire at temperatures above and below the LCST of the microgels. At 20 °C, the water droplet adopts a barrel-like configuration (Fig. 10a). Barrel-like configurations indicate a more hydrophilic

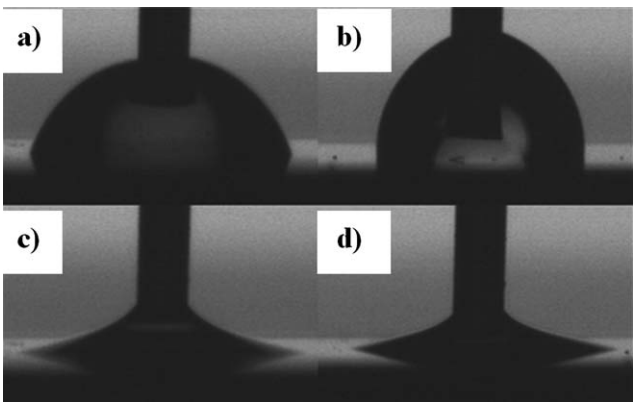

Fig. 9 Advancing (a and b) and receding (c and d) contact angle snapshots. (a) Image taken at 23 °C. Advancing contact angle was calculated to be 71 ± 2°. (b) Image was taken at 50 °C. Advancing contact angle was calculated to be 90 ± 2°. (c) Image was taken at 23 °C. Receding contact angle was calculated to be 13 ± 2°. (d) Image was taken at 50 °C. Receding contact angle was taken to be 13 ± 2°.

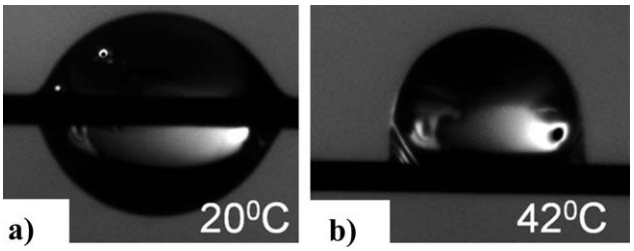

Fig. 10 Optical images of the water droplet on the tungsten wire modified with the grafted microgel layer at different temperatures: (a): barrel-like configuration; (b): clamshell-like configuration.

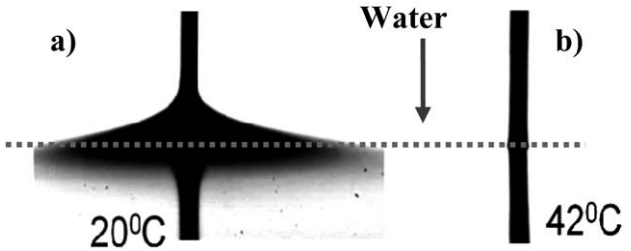

Fig. 11 Change of the wettability of the tungsten wire grafted with a microgel layer, inserted in water of different temperatures.

surface in nature.[82] This is because the liquid has a greater affinity to the surface, which creates a larger area of interaction between the water and modified wire. Using the image analysis based on the Carroll formulas[83] the contact angle was estimated as ~40°. Contrarily, the drop adopts a clam-shell configuration when placed on the warm wire maintained at 42 °C (Fig. 10b). This is a manifestation of its weak wettability. Typically, the drop forms the clam-shell-like configuration at contact angles of greater than 70°, which indicates that the surface is less hydrophilic.[82] It was also established that the quantitative wetting data significantly depends on the method of measurements. Fig. 11a shows the meniscus formed when a modified tungsten wire is immersed perpendicularly into the 20 °C water. Again, we observe a meniscus that crawls up the side of the wire, confirming that the wire surface is wettable. Using the image analysis based on the Lo formulas,[84] the contact angle was estimated to be ~14°, *i.e.* it is much smaller than that found for a droplet. When the temperature was raised up to 40 °C which is above the LCST of the PNIPAM microgels, the meniscus configuration changed significantly, Fig. 11b. It became virtually flat, practically perpendicular to the immersed wire. This change directly indicates a change in the surface energy, as this configuration suggests a more hydrophobic surface. The results obtained for the tungsten wires suggest that the grafted microgel layer retains its ability to change morphologically when exposed to external temperature variations on both flat and more complex, curved surfaces.

Conclusions

The PNIPAM-containing thermoresponsive microgels with carboxy functionalities were synthesized *via* a surfactant-stabilized, free-radical, precipitation polymerization in an aqueous environment in the presence of acrylic acid as a co-monomer and BIS as a cross-linker. Analyses indicated that the particles were composed of a densely cross-linked core containing a high ratio of AAc and BIS, and a shell comprising mostly NIPAM "hairs." A monolayer of the thermoresponsive microgel PNIPAM nanoparticles was grafted onto the surface of silicon wafers, glass slides, PVDF fibers, and tungsten wires. Particle anchoring was conducted by the "grafting to" approach using a PGMA anchoring layer. AFM and SEM studies demonstrated that the grafted layer covered the surfaces uniformly at the microscopic level. The grafted monolayer swelled and collapsed reversibly at temperatures below and above the LCST of the PNIPAM. For the flat silicon substrate, a wettability study of the grafted layer showed ~20° increase in the water advancing contact angle upon heating above the LCST of the PNIPAM. A significant hysteresis exists between the advancing and receding angles, and wettability experiments indicated that the receding angle is virtually independent of temperature for this system. The wettability data obtained for the tungsten wires show that the grafted microgel layer retains its ability to undergo morphological changes when exposed to external temperature variations on complex curved surfaces. Overall, the results obtained demonstrate that, in many aspects, the grafted microgel layer, as a system, is comparable in performance to a PNIPAM brush system with respect to their thermoresponsive properties.

Acknowledgements

The research presented has been supported by the National Science Foundation grants CMMI-0826067 and CMMI-0825773, and the U.S. Air Force contract FA8650-09-D-5900.

Notes and references

1 I. Luzinov, S. Minko and V. V. Tsukruk, *Soft Matter*, 2008, **4**, 714–725.
2 M. A. Cohen Stuart, W. T. S. Huck, J. Genzer, M. Muller, C. Ober, M. Stamm, G. B. Sukhorukov, I. Szleifer, V. V. Tsukruk, M. Urban, F. Winnik, S. Zauscher, I. Luzinov and S. Minko, *Nat. Mater.*, 2010, **9**, 101–113.
3 K. Nagase, J. Kobayashi and T. Okano, *J. R. Soc. Interface*, 2009, **6**, S293–S309.
4 D. Crespy and R. N. Rossi, *Polym. Int.*, 2007, **56**, 1461–1468.
5 I. Dimitrov, B. Trzebicka, A. H. E. Muller, A. Dworak and C. B. Tsvetanov, *Prog. Polym. Sci.*, 2007, **32**, 1275–1343.
6 F. Ercole, T. P. Davis and R. A. Evans, *Polym. Chem.*, 2010, **1**, 37–54.
7 J. S. Katz and J. A. Burdick, *Macromol. Biosci.*, 2010, **10**, 339–348.
8 D. M. He, H. Susanto and M. Ulbricht, *Prog. Polym. Sci.*, 2009, **34**, 62–98.
9 T. Seki, *Curr. Opin. Solid State Mater. Sci.*, 2006, **10**, 241–248.
10 M. R. Bohmer, A. L. Klibanov, K. Tiemann, C. S. Hall, H. Gruell and O. C. Steinbach, *Eur. J. Radiol.*, 2009, **70**, 242–253.
11 H. Meng and J. L. Hu, *J. Intell. Mater. Syst. Struct.*, 2010, **21**, 859–885.
12 C. S. Brazel, *Pharm. Res.*, 2009, **26**, 644–656.
13 T. Y. Liu, S. H. Hu, D. M. Liu, S. Y. Chen and I. W. Chen, *Nano Today*, 2009, **4**, 52–65.
14 S. Dai, P. Ravi and K. C. Tam, *Soft Matter*, 2008, **4**, 435–449.
15 A. Richter, G. Paschew, S. Klatt, J. Lienig, K. F. Arndt and H. J. P. Adler, *Sensors*, 2008, **8**, 561–581.
16 B. Jeong and A. Gutowska, *Trends Biotechnol.*, 2002, **20**, 305–311.
17 V. Tsyalkovsky, R. Burtovyy, V. Klep, R. Lupitskyy, M. Motornov, S. Minko and I. Luzinov, *Langmuir*, 2010, **26**, 10684–10692.
18 O. Hoy, B. Zdyrko, R. Lupitskyy, R. Sheparovych, D. Aulich, J. F. Wang, E. Bittrich, K. J. Eichhorn, P. Uhlmann, K. Hinrichs,

Published on 30 August 2011 on http://pubs.rsc.org | doi:10.1039/C1SM05924F
Downloaded by Clemson University on 29 December 2011

This journal is © The Royal Society of Chemistry 2011

View Online

M. Muller, M. Stamm, S. Minko and I. Luzinov, *Adv. Funct. Mater.*, 2010, **20**, 2240–2247.
19 T. Okano, N. Yamada, M. Okuhara, H. Sakai and Y. Sakurai, *Biomaterials*, 1995, **16**, 297–303.
20 A. J. Convertine, N. Ayres, C. W. Scales, A. B. Lowe and C. L. McCormick, *Biomacromolecules*, 2004, **5**, 1177–1180.
21 D. M. Jones, J. R. Smith, W. T. S. Huck and C. Alexander, *Adv. Mater.*, 2002, **14**, 1130–1134.
22 J. E. Chung, M. Yokoyama, T. Aoyagi, Y. Sakurai and T. Okano, *J. Controlled Release*, 1998, **53**, 119–130.
23 Y. Xia, N. A. D. Burke and H. D. H. Stover, *Macromolecules*, 2006, **39**, 2275–2283.
24 Y. V. Pan, R. A. Wesley, R. Luginbuhl, D. D. Denton and B. D. Ratner, *Biomacromolecules*, 2001, **2**, 32–36.
25 T. Yakushiji, K. Sakai, A. Kikuchi, T. Aoyagi, Y. Sakurai and T. Okano, *Langmuir*, 1998, **14**, 4657–4662.
26 Y. Ito, G. P. Chen, Y. Q. Guan and Y. Imanishi, *Langmuir*, 1997, **13**, 2756–2759.
27 J. E. Chung, M. Yokoyama, K. Suzuki, T. Aoyagi, Y. Sakurai and T. Okano, *Colloids Surf., B*, 1997, **9**, 37–48.
28 J. Jhang, R. Pelton and Y. L. Deng, *Langmuir*, 1995, **11**, 2301–2302.
29 M. C. LeMieux, S. Peleshanko, K. D. Anderson and V. V. Tsukruk, *Langmuir*, 2006, **23**, 265–273.
30 M. E. Harmon, D. Kuckling and C. W. Frank, *Macromolecules*, 2003, **36**, 162–172.
31 D. Kuckling, M. E. Harmon and C. W. Frank, *Macromolecules*, 2002, **35**, 6377–6383.
32 X. Huang, G. P. Misra, A. Vaish, J. M. Flanagan, B. Sutermaster and T. L. Lowe, *Macromolecules*, 2008, **41**, 8339–8345.
33 D. Kuckling, C. D. Vo and S. E. Wohlrab, *Langmuir*, 2002, **18**, 4263–4269.
34 J. T. Zhang, X. L. Liu, A. Fahr and K. D. Jandt, *Colloid Polym. Sci.*, 2008, **286**, 1209–1213.
35 D. Kuckling, *Colloid Polym. Sci.*, 2009, **287**, 881–891.
36 L. A. Lyon, Z. Y. Meng, N. Singh, C. D. Sorrell and A. S. John, *Chem. Soc. Rev.*, 2009, **38**, 865–874.
37 I. Tokarev and S. Minko, *Soft Matter*, 2009, **5**, 511–524.
38 I. Luzinov, S. Minko and V. V. Tsukruk, *Prog. Polym. Sci.*, 2004, **29**, 635–698.
39 B. Zhao and W. J. Brittain, *Prog. Polym. Sci.*, 2000, **25**, 677–710.
40 A. T. ten Cate, S. A. F. Reinders, D. H. Turkenburg, A. Bruin, F. D'Souza, G. T. Donnelly, P. R. Willemsen, J. H. Maas and K. J. C. van Bommel, *Prog. Org. Coat.*, 2009, **64**, 221–224.
41 K. S. Iyer, B. Zdyrko, H. Malz, J. Pionteck and I. Luzinov, *Macromolecules*, 2003, **36**, 6519–6526.
42 N. C. Estillore, J. Y. Park and R. C. Advincula, *Macromolecules*, 2010, **43**, 6588–6598.
43 R. A. L. Jones, R. J. Lehnert, H. Schonherr and J. Vancso, *Polymer*, 1999, **40**, 525–530.
44 M. Kaholek, W. K. Lee, S. J. Ahn, H. W. Ma, K. C. Caster, B. LaMattina and S. Zauscher, *Chem. Mater.*, 2004, **16**, 3688–3696.
45 E. Bittrich, M. Kuntzsch, K. J. Eichhorn and P. Uhlmann, *J. Polym. Sci., Part B: Polym. Phys.*, 2010, **48**, 1606–1615.
46 S. Balamurugan, S. Mendez, S. S. Balamurugan, M. J. O'Brien and G. P. Lopez, *Langmuir*, 2003, **19**, 2545–2549.
47 K. N. Plunkett, X. Zhu, J. S. Moore and D. E. Leckband, *Langmuir*, 2006, **22**, 4259–4266.
48 S. Schmidt, M. Zeiser, T. Hellweg, C. Duschl, A. Fery and H. Mohwald, *Adv. Funct. Mater.*, 2010, **20**, 3235–3243.
49 L. Ying, E. T. Kang and K. G. Neoh, *Langmuir*, 2002, **18**, 6416–6423.
50 R. M. P. Da Silva, J. F. Mano and R. L. Reis, *Trends Biotechnol.*, 2007, **25**, 577–583.
51 J. Jagur-Grodzinski, *Polym. Adv. Technol.*, 2010, **21**, 27–47.
52 M. Hamidi, A. Azadi and P. Rafiei, *Adv. Drug Delivery Rev.*, 2008, **60**, 1638–1649.
53 S. Kim, J. H. Kim, O. Jeon, I. C. Kwon and K. Park, *Eur. J. Pharm. Biopharm.*, 2009, **71**, 420–430.
54 Q. S. Zhang, L. S. Zha, J. H. Ma and B. R. Liang, *J. Colloid Interface Sci.*, 2009, **330**, 330–336.
55 J. Rieger, C. Grazon, B. Charleux, D. Alaimo and C. Jerome, *J. Polym. Sci., Part A: Polym. Chem.*, 2009, **47**, 2373–2390.
56 H. X. Liu, C. Y. Wang, Q. X. Gao, X. X. Liu and Z. Tong, *Acta Biomater.*, 2010, **6**, 275–281.
57 P. A. FitzGerald, D. Dupin, S. P. Armes and E. J. Wanless, *Soft Matter*, 2007, **3**, 580–586.
58 M. Horecha, V. Senkovskyy, A. Synytska, M. Stamm, A. I. Chervanyov and A. Kiriy, *Soft Matter*, 2010, **6**, 5980–5992.
59 B. Zdyrko, K. S. Iyer and I. Luzinov, *Polymer*, 2006, **47**, 272–279.
60 B. Zdyrko, O. Hoy, M. K. Kinnan, G. Chumanov and I. Luzinov, *Soft Matter*, 2008, **4**, 2213–2219.
61 O. Burtovyy, V. Klep, H. C. Chen, R. K. Hu, C. C. Lin and I. Luzinov, *J. Macromol. Sci., Part B: Phys.*, 2007, **46**, 137–154.
62 V. Tsyalkovsky, V. Klep, K. Ramaratnam, R. Lupitskyy, S. Minko and I. Luzinov, *Chem. Mater.*, 2008, **20**, 317–325.
63 X. Li, J. Zuo, Y. L. Guo and X. H. Yuan, *Macromolecules*, 2004, **37**, 10042–10046.
64 N. Singh, S. M. Husson, B. Zdyrko and I. Luzinov, *J. Membr. Sci.*, 2005, **262**, 81–90.
65 M. L. Christensen and K. Keiding, *Colloids Surf., A*, 2005, **252**, 61–69.
66 R. H. Pelton and P. Chibante, *Colloids Surf.*, 1986, **20**, 247–256.
67 B. E. Rodriguez, M. S. Wolfe and M. Fryd, *Macromolecules*, 1994, **27**, 6642–6647.
68 B. R. Saunders, *Langmuir*, 2004, **20**, 3925–3932.
69 T. G. Mason and M. Y. Lin, *Phys. Rev. E: Stat., Nonlinear, Soft Matter Phys.*, 2005, **71**, 040801.
70 M. Stieger, J. S. Pedersen, P. Lindner and W. Richtering, *Langmuir*, 2004, **20**, 7283–7292.
71 A. Fernandez-Barbero, A. Fernandez-Nieves, I. Grillo and E. Lopez-Cabarcos, *Phys. Rev. E: Stat. Phys., Plasmas, Fluids, Relat. Interdiscip. Top.*, 2002, **66**, 051803.
72 X. Wu, R. H. Pelton, A. E. Hamielec, D. R. Woods and W. McPhee, *Colloid Polym. Sci.*, 1994, **272**, 467–477.
73 O. Burtovyy, V. Klep, T. Turel, Y. Gowayed and I. Luzinov, Polymeric Membranes: Surface Modification by "Grafting to" Method and Fabrication of Multilayered Assemblies, in *Nanoscience and Nanotechnology for Chemical and Biological Defense*, ed. R. Nagarajan, W. Zukas, T. A. Hatton and S. Lee, ACS Symposium Series 1016, Washington DC, 2009.
74 B. Zdyrko, V. Klep and I. Luzinov, *Mater. Matters (Milwaukee, WI, U. S.)*, 2008, **3**, 44–47.
75 I. A. Luzinov, K. L. Swaminatha Iyer, V. Z. Klep and B. V. Zdyrko, *US pat.*, 7 026 014 B2, Clemson University, USA, April 11, 2006, p. 33.
76 B. Zdyrko and I. Luzinov, *Macromol. Rapid Commun.*, 2011, 32, 859–869.
77 S. Schmidt, T. Hellweg and R. von Klitzing, *Langmuir*, 2008, **24**, 12595–12602.
78 S. Schmidt, H. Motschmann, T. Hellweg and R. von Klitzing, *Polymer*, 2008, **49**, 749–756.
79 V. Klep, B. Zdyrko and I. Luzinov, *PMSE Prepr.*, 2005, **93**, 462.
80 S. Hofl, L. Zitzler, T. Hellweg, S. Herminghaus and F. Mugele, *Polymer*, 2007, **48**, 245–254.
81 L. Liang, X. D. Feng, J. Liu, P. C. Rieke and G. E. Fryxell, *Macromolecules*, 1998, **31**, 7845–7850.
82 G. McHale and M. I. Newton, *Colloids Surf., A*, 2002, **206**, 79–86.
83 B. J. Carroll, *J. Colloid Interface Sci.*, 1976, **57**, 488–495.
84 L. L. Lo, *J. Fluid Mech.*, 1973, **132**, 65–78.

Published on 30 August 2011 on http://pubs.rsc.org | doi:10.1039/C1SM05924F
Downloaded by Clemson University on 29 December 2011